Efficient iterative reconstruction for parallel MRI in strongly inhomogeneous B_0

C. Barmet[1], J. Tsao[1], K.P. Pruessmann[1]

[1]*Institute for Biomedical Engineering, University and ETH Zurich*

INTRODUCTION:

In MRI, inhomogeneity of the main magnetic field B_0 causes significant shifts and distortions when the field variations are large compared to the pixel bandwidth. This is frequently the case at high field strength and with long read-out trains such as in echo-planar and spiral or high resolution imaging. At the reconstruction level, the problem of B_0 inhomogeneity is typically addressed by unwarping (1) or conjugate phase reconstruction (2,3,4). However, the conjugate phase approach relies on the assumption that B_0 varies smoothly in space. Recently, iterative solutions were suggested which can cope with strongly varying B_0 (5, 6). They are based on the conjugate gradient (CG) algorithm, which has also been employed for SENSE reconstruction (7).

In the present work we describe the generalization of iterative B_0-corrected reconstruction toward parallel imaging.

METHODS:

The problem of compensating for in-plane B_0 inhomogeneity in the reconstruction is frequently badly conditioned, leading to numerical instability and local noise enhancement. To address this problem, it has been proposed (6) to minimize the weighted sum of the noise variance and the expected squared signal error on a pixel-by pixel basis. This is achieved with the reconstruction formula

$$\mathbf{I} = \beta\theta E^H(\beta E\theta E^H + \alpha\psi)^+ \mathbf{m} \qquad (1)$$

where $\mathbf{m}$ is a vector of multiple-coil k-space data, $\mathbf{I}$ the vector of the reconstructed pixel values, E the encoding matrix and E^H its Hermitian adjoint. The superscript + denotes the Moore-Penrose pseudoinverse. α and β are coefficients representing the weight of noise and signal variance, respectively, in the joint minimization. Ψ denotes the noise covariance of the sample values and θ denotes the signal covariance, which represents potential prior knowledge about the signal distribution in the object. No prior knowledge corresponds to θ equal to identity. Note that the set of target pixel positions can be arbitrarily large, corresponding to an arbitrary target resolution. For the particular case of sensitivity- and Fourier encoding under the influence of B_0 inhomogeneity, the encoding matrix reads

$$E_{\kappa,\rho,\gamma} = s_\gamma(\mathbf{r}_\rho)\exp(-i\mathbf{k}_\kappa\mathbf{r}_\rho - i\omega_\rho t_\kappa), \qquad (2)$$

where $\mathbf{k}_\kappa$ and $\mathbf{r}_\rho$ denote the κ-th sampling position in k-space and the position of the ρ-th pixel in the image domain, respectively. ω_ρ denotes the B_0-induced frequency offset at the position $\mathbf{r}_\rho$, and t_κ denotes the time at which the sample κ is taken. The sensitivity of coil γ at position $\mathbf{r}_\rho$ is given by $s_\gamma(\mathbf{r}_\rho)$. For image reconstruction with Eq. (1), the matrix inversion part is solved by the CG method. Its solution $\mathbf{x}$ can then be pre-multiplied by the left-most part of Eq. (1) to get the reconstructed image: $\mathbf{I}=\beta\theta E^H\mathbf{x}$. The efficiency of each loop in the CG scheme (cf. Fig.2) can be enhanced considerably (6) by performing the matrix-vector multiplications with E and E^H by combining multifrequency interpolation (MFI) (4) with fast Fourier transform, in a scheme related to an approach proposed in Ref. (7) (cf. Figs.1&2). If noise correlation between the coils is significant, this can be addressed by creating virtual receiver channels as proposed in (7).

The performance of the proposed method was assessed in a simulation study. For data construction a spherical homogeneous object, four typical coil sensitivities and a massively inhomogeneous B0-map (ranging from -1360Hz to 900Hz) were constructed on a high resolution grid. A Spin-echo sequence with low readout bandwidth was assumed to create pronounced B_0. The k-space data was obtained by applying the adjoint of the MFI (Fig. 1) to the object and undersampling the data discarding every second line. α and β were chosen such as to yield approximately identical noise and artifact levels. θ was set to a diagonal matrix, with ones for pixels inside the (slightly extended) object and zeroes elsewhere.

RESULTS:

The measured data was reconstructed using standard DFT reconstruction, conventional MFI, and the proposed reconstruction (50 iterations, reconstructed on a 512x512 grid, 3 hours computation on a 2.8 GHz CPU). MFI recovers the original shape of the phantom. However the aliased portions in the MFI image remain distorted. This illustrates that straight forward SENSE unfolding will not work in this case. Furthermore, MFI yields a false intensity distribution.

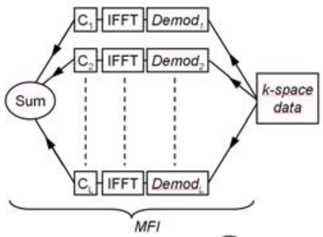

Fig. 1: In MFI the k-space data is demodulated at L different frequencies ($Demod_i$), inverse Fourier transformed and multiplied by the corresponding coefficient maps (C_i) before being summed up.

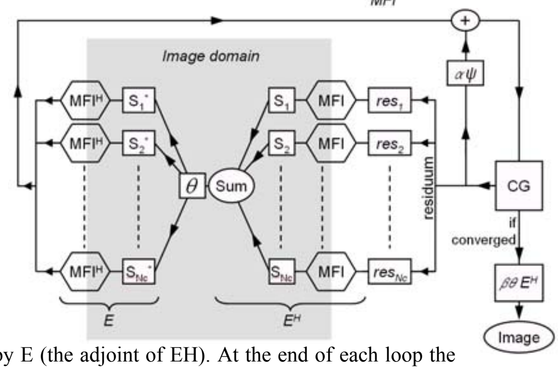

Fig 2: One iteration of the CG loop is shown where the residual (computed by CG) for every coil is treated by MFI before being multiplied by the sensitivity map of the respective coil (S_i). After the multiplication with θ the data is multiplied by E (the adjoint of EH). At the end of each loop the original residual, multiplied by $\alpha\Psi$, is added for regularization.

The proposed algorithm yielded an accurate image free of aliasing and erroneous intensity variation. In particular unlike MFI it does not assign excessive signal close to the region of strongest B_0-variation.

DISCUSSION AND CONCLUSION:

The proposed method permits robust, efficient B_0-corrected reconstruction of sensitivity-encoded data without restrictions in terms of local B_0 variation. The reconstruction scheme is readily applicable to general k-space trajectories, suggesting promising applications in fMRI and DTI. Ultimately, the reconstruction is limited by the inherent information content of the acquired data. Excessive field inhomogeneity will cause deteriorating conditioning, shifting the balance in the weighted minimization toward unfavorable compromises of the spatial response

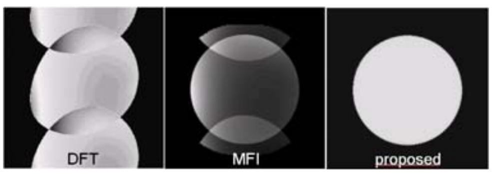

Fig. 3: Comparison of different reconstructions

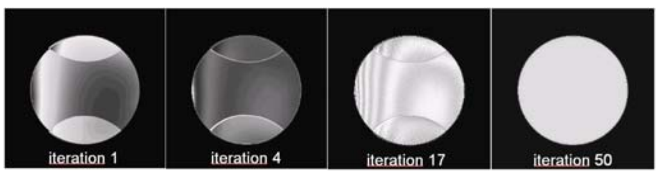

Fig. 4: For the proposed reconstruction, the results after 1, 4, 17 and 50 iterations is shown.

REFERENCES:

[1] Jezzard, P. et al, MRM 34:65-73(1995), [2] Maeda, A. et al, IEEE TMI 7:26-31 (1988), [3] Noll, D. et al, IEEE TMI 10:629-37, [4] Man, L.-C. et al, MRM 37:785-792 (1997), [5] Sutton, B. et al, Proc. ISMRM 2001, p. 771, [6] Barmet, C. et al, Proc. ISMRM 2004, p. 80, [7] Pruessmann, K.P. et al, MRM 46:638-51 (2001).